

Computational Light-Field Microscopy and an Application in Neuroscience

Pier Luigi Dragotti

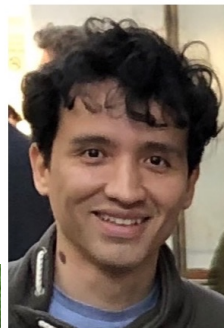
Joint work with



Pingfan Song



Carmel Howe



Herman Verinaz



Amanda Foust



Peter Quicke

- Multi-photon microscopy and neuroscience
- The image formation process in light-field microscopy (LFM)
- Volume reconstruction
 - Discretization of the forward model
 - Reconstruction based on ADMM
 - On going work: extension of the model-based approaches to deep learning via unfolding
- Localization of neurons using LFM
 - EPI structure and EPI dictionary
 - Localization based on convolutional sparse coding
 - On going work: extension of the model-based approaches to deep learning via unfolding
- Conclusions

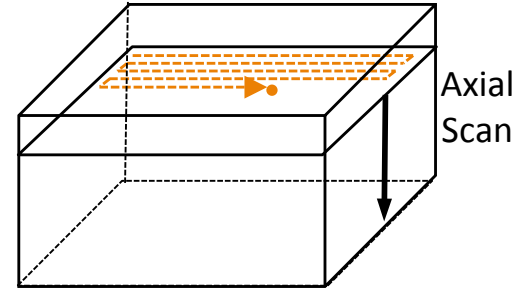
Two-Photon Microscopy for Neuroscience

- Goal of Neuroscience: to study how information is processed in the brain
- Neurons communicate through pulses called Action Potentials (AP)
- Need to measure in-vivo the activity of large populations of neurons at cellular level resolution
- Two-photon microscopy combined with right indicators is the most promising technology to achieve that

Two-Photon Microscopy

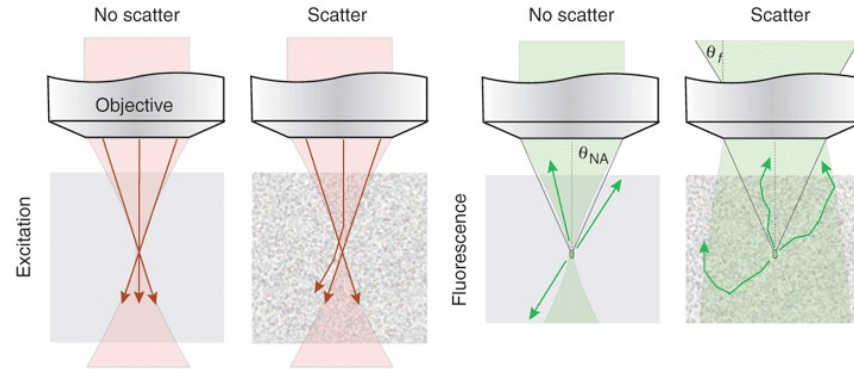
- Fluorescent sensors within tissues
- Highly localized laser excites fluorescence from sensors
- Photons emitted from tissue are collected
- Focal spot sequentially scanned across samples to form image

Point scanning (2PLSM)



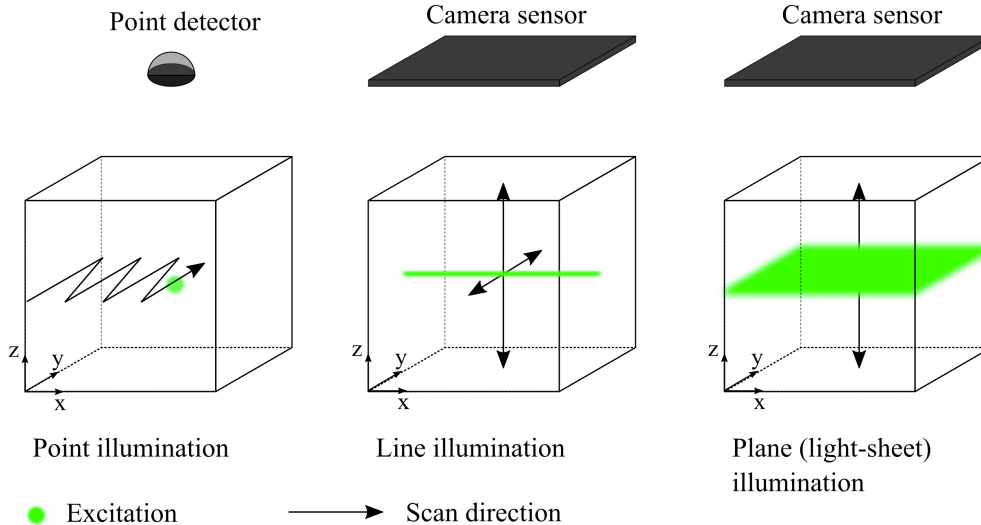
Two-Photon Microscopy

- Fluorescent sensors within tissues
- Highly localized laser excites fluorescence from sensors
- Photons emitted from tissue are collected
- Focal spot sequentially scanned across samples to form image
- Two-photon microscopes in raster scan modality can go deep in the tissue but are **slow**



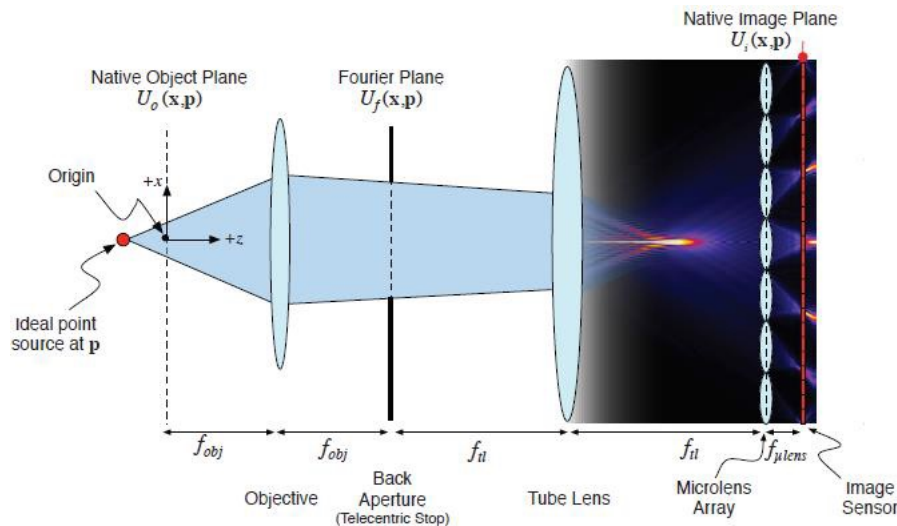
Two-Photon Microscopy

- In order to speed up acquisition one can change the illumination strategy
- This mitigates the issue but does not fix it

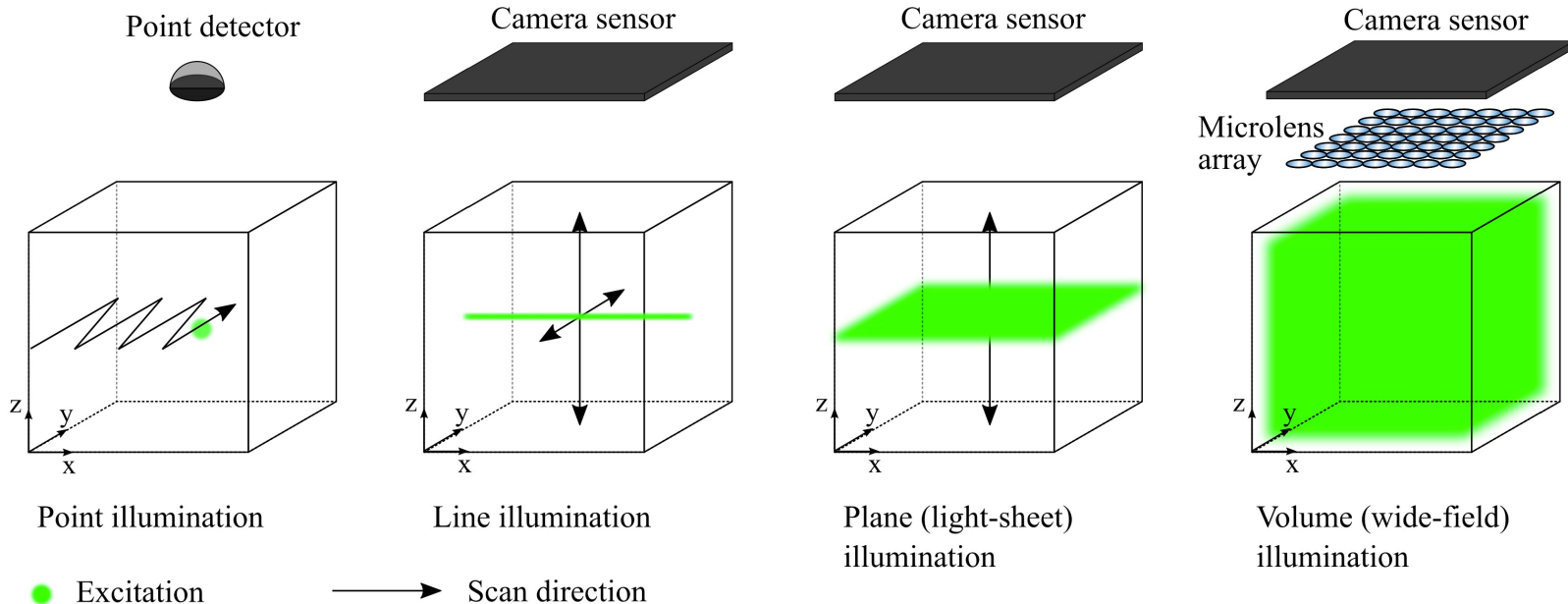


Light-field Microscopy

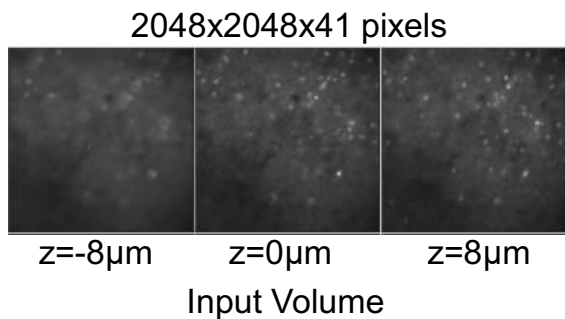
Light-Field Microscopy (LFM) is a high-speed (scan-less) imaging technique that uses a simple modification of a standard microscope to capture a 3D image of an entire volume in a single camera snapshot



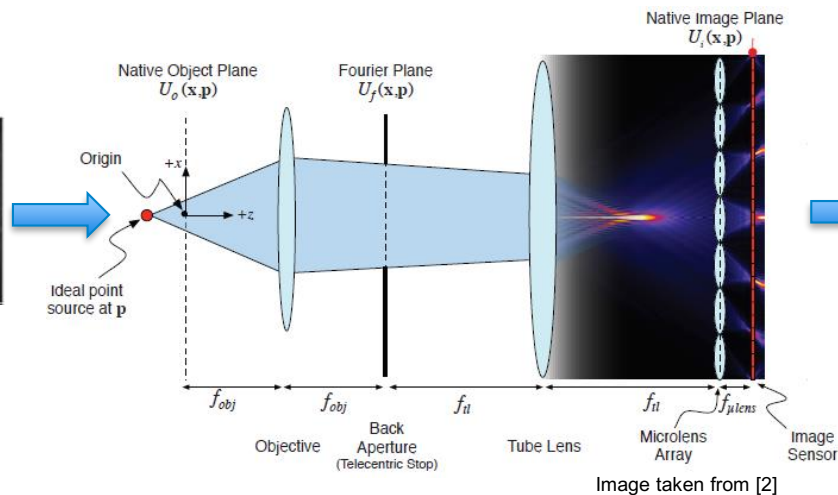
Light-field Microscopy and Illumination Strategies



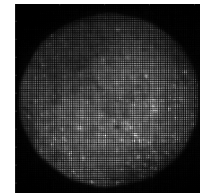
Light-field Microscopy



Brain slice (50 μm thick) taken from a GFP Tagged triple transgenic mouse line using our light field microscope

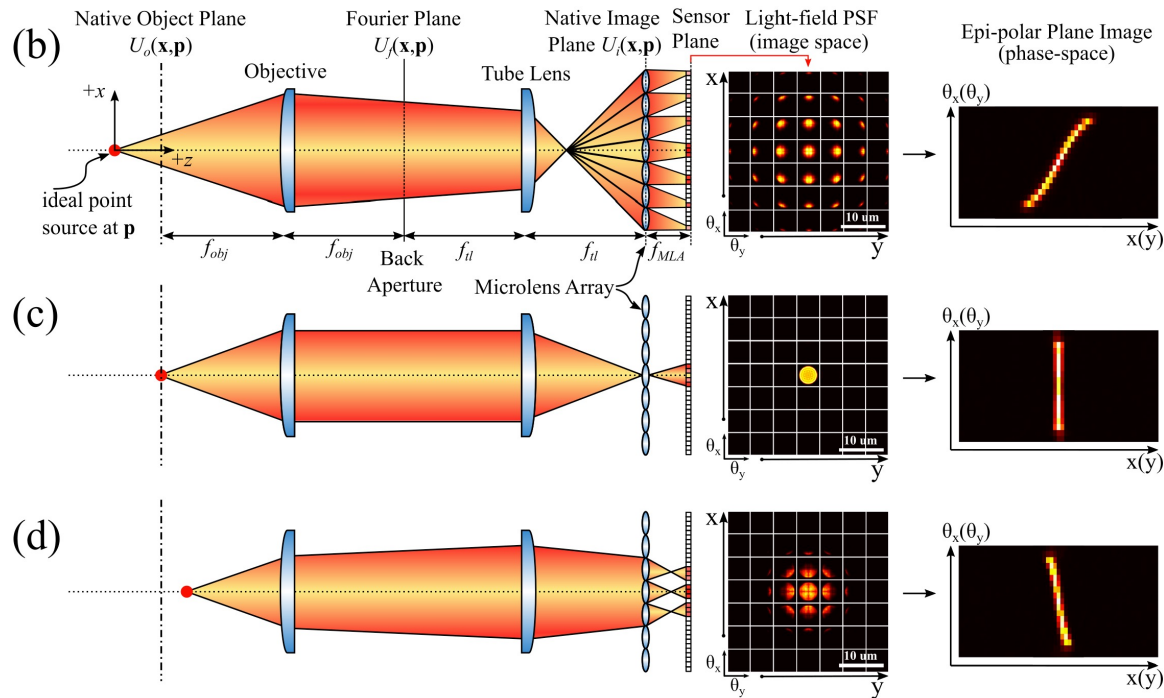
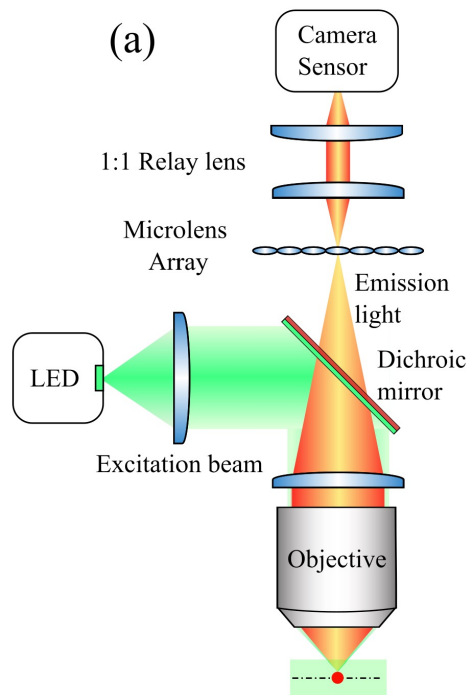


2048x2048 pixels



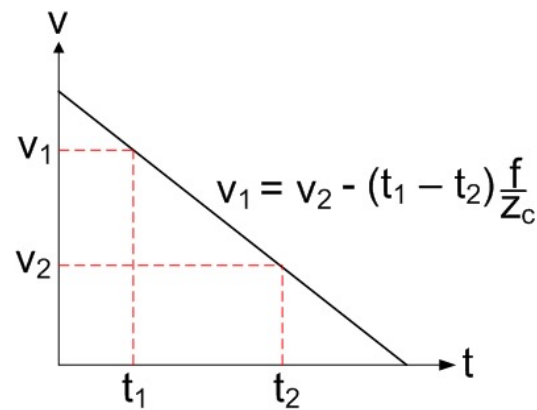
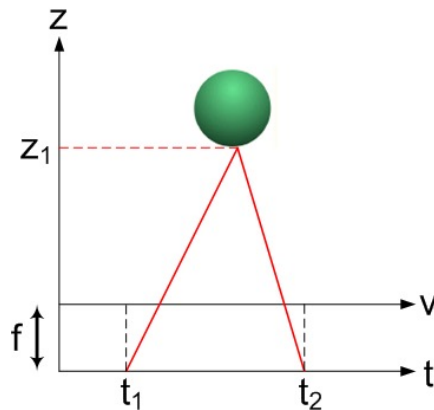
Measured LF

Light-field Microscopy



Epipolar Plane Image (EPI)

- Taking one slice of the lightfield leads to the EPI
- Points are mapped onto lines in the (EPI)
- Slope of lines are inversely proportional to the depth
- Lines with larger slopes occlude lines with smaller slopes

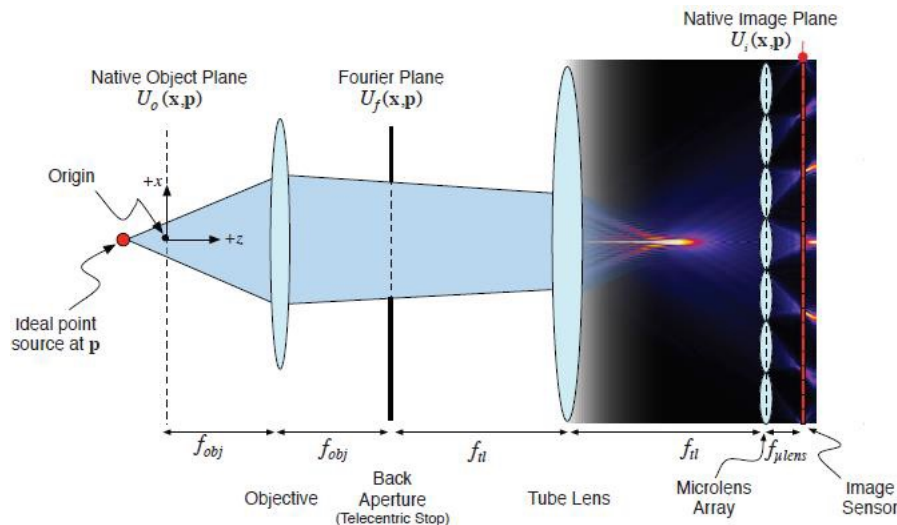


IBR Results on the Lightfield



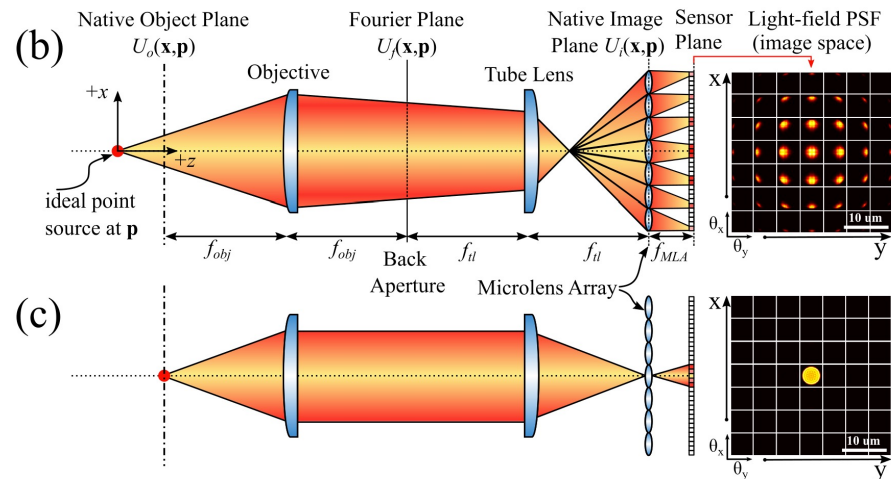
Light-field Microscopy

- Challenges
 - Cannot use ray approximation (**geometric optics**) to model the image formation. Need to use **wave optics**
 - Scattering induces blur, making inversion more challenging
- Opportunities
 - Data is **sparse** (neurons fire rarely and are localized in space)
 - Occlusion can be ignored
 - **Localization** of neurons is often sufficient (no need for high-quality volume reconstruction)



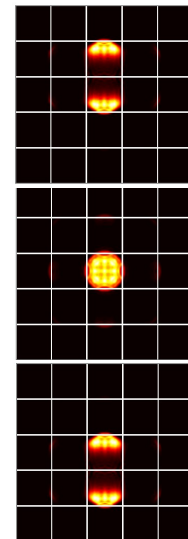
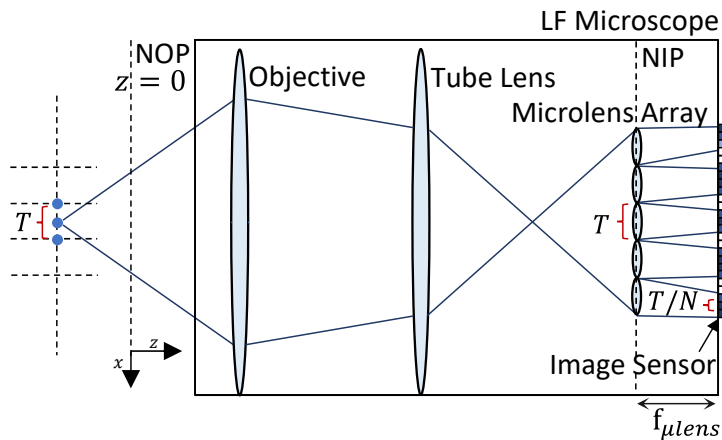
Light-field Microscopy – Wave Model

- Wave Optics model [Broxton et al. 2013]
- Based on estimating the wavefront at three specific points:
 - Use Debye theory to compute the wavefront at NIP
 - Microlens array (MLA) then makes the PSF periodically shift invariant
 - Use Fresnel diffraction solution to estimate the wavefront at the sensor plane



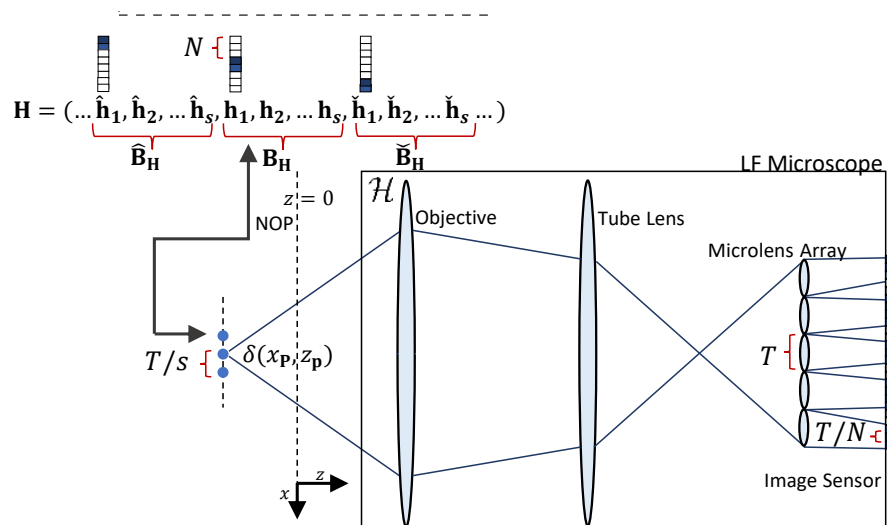
Light-field Microscopy – Wave Model

- Wave Optics model [Broxton et al. 2013]
- Based on estimating the wavefront at three specific points:
 - Use Debye theory to compute the wavefront at NIP
 - Microlens array (MLA) then makes the PSF periodically shift invariant
 - Use Fresnel diffraction solution to estimate the wavefront at the sensor plane



Discretization of the Forward Model

- Given the expression of the wavefront per point source
- The PSF $h(\mathbf{p}, x)$ is discretized by shifting the point source along a grid and by storing the sampled light-field pattern. This leads to the discrete system $\mathbf{g} = \mathbf{H}\mathbf{f}$
- Issue:
 - the signal might be better modelled using an elementary function different from a Dirac
 - Dependency across depths not exploited
 - Blocking artefacts at the native object plane

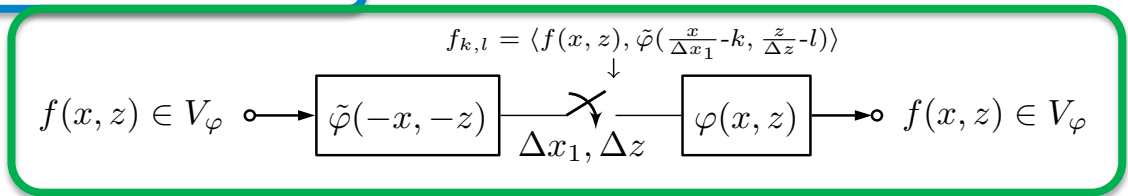


- Given $\mathbf{g} = \mathbf{H}\mathbf{f}$ reconstruction of \mathbf{f} can be problematic
 - \mathbf{H} is ill-conditioned
 - Note that \mathbf{H} is block-circulant (periodically shift invariant) and can be modelled with a filter-bank
- Approach:
 - Use generalized sampling theory to improve the discretization
 - Use SVD to simplify the forward model
 - Inversion based on stronger priors and ADMM

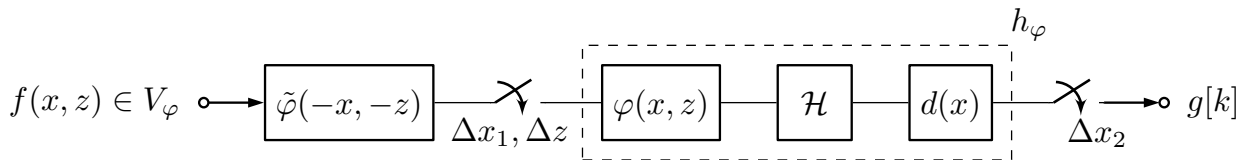
Discretization of Forward Model

- New discretization
 - $f(x, z)$ is assumed to belong to a shift-invariant space generated by $\varphi(x, z)$:

$$f(x, z) = \sum_{k,l} f_{k,l} \varphi(x - k, z - l) \text{ where } f_{k,l} = \langle f(x, z), \tilde{\varphi}(x - k, z - l) \rangle$$

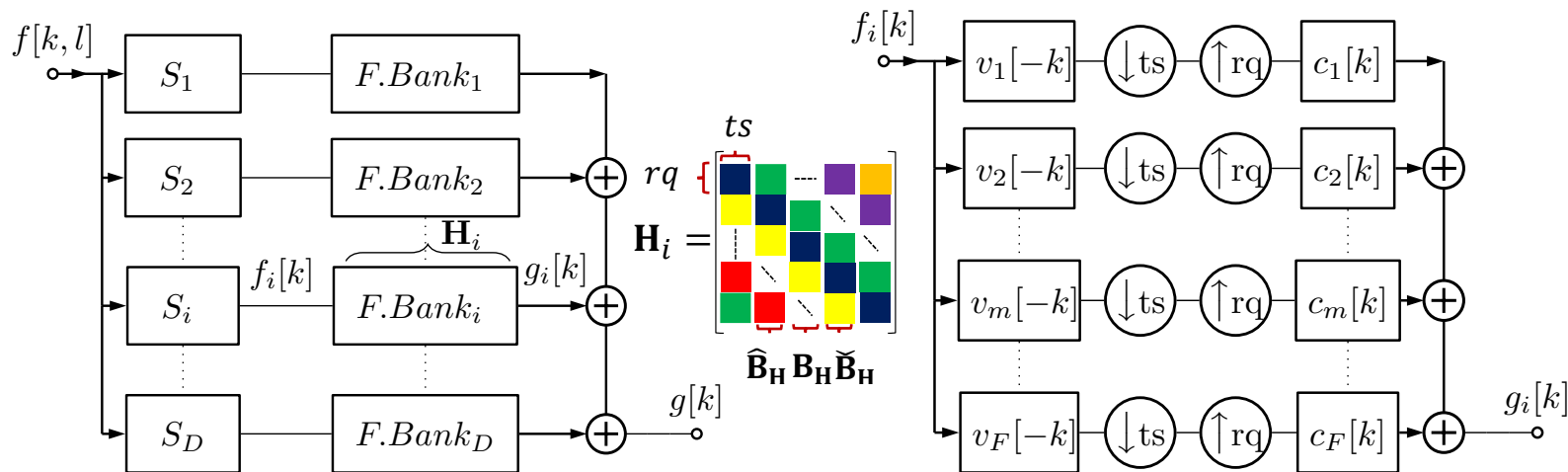


- We use linear splines as $\varphi(x, z)$. This leads to a new better-conditioned H



Discretization of Forward Model

- The forward model is periodically shift invariant and so can be modelled with a filter-bank

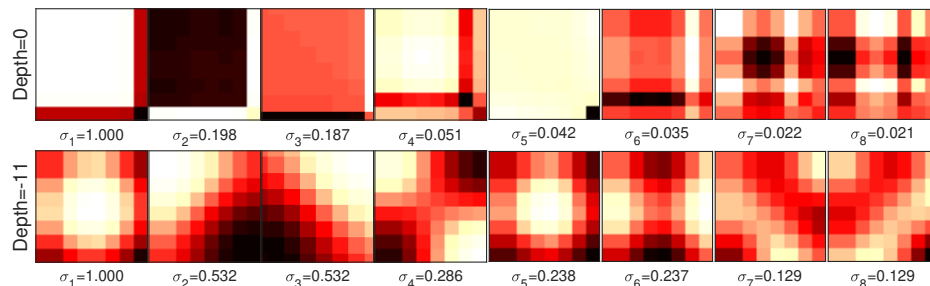


Discretization of Forward Model

- The new filters related to H are more stable:

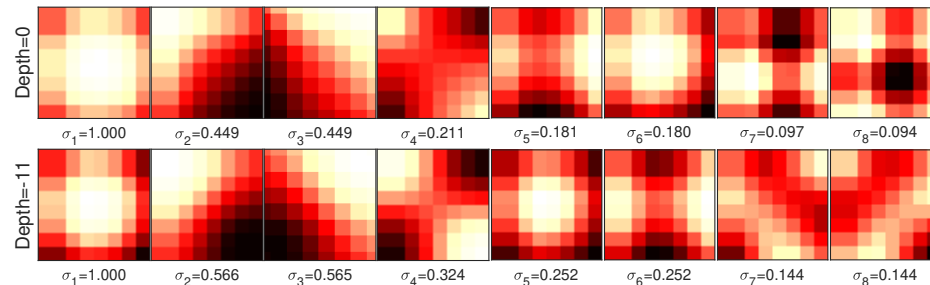
Old discretization

a)



New discretization

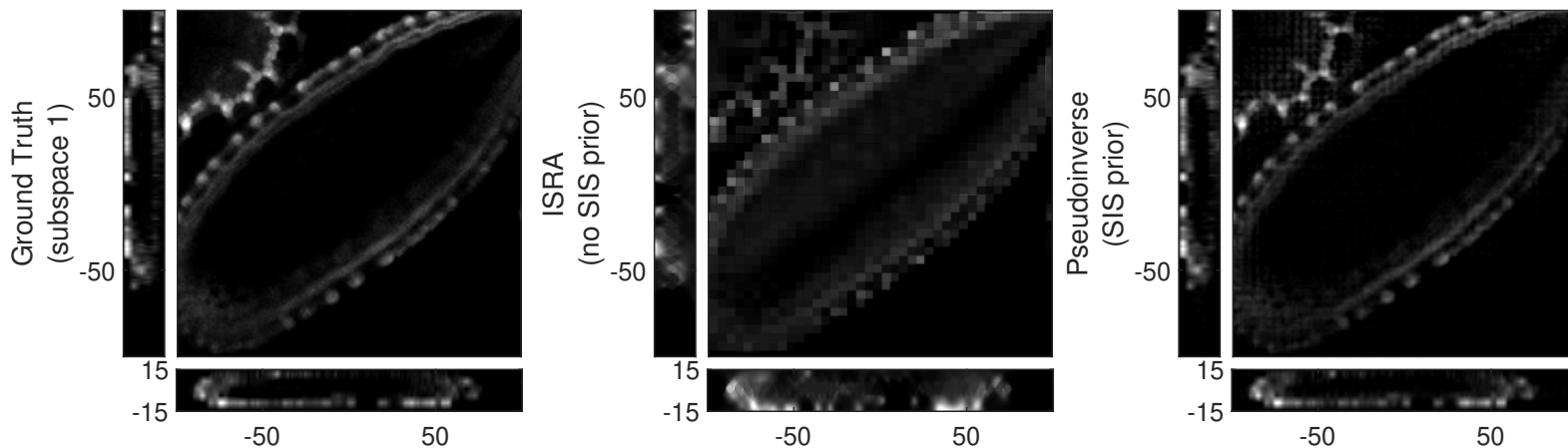
b)



Volume Reconstruction from LF Data

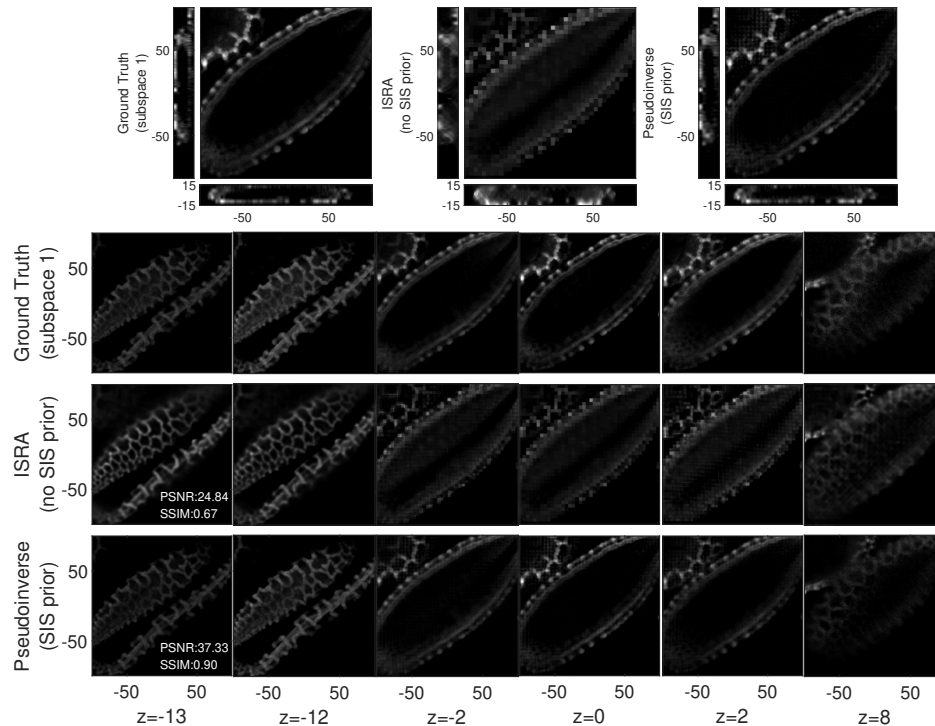
- “Linear” reconstruction with the new forward model does not suffer from blocking artefacts:

$$g = Hf$$



Volume Reconstruction from LF Data

- “Linear” reconstruction with the new forward model does not suffer from blocking artefacts:

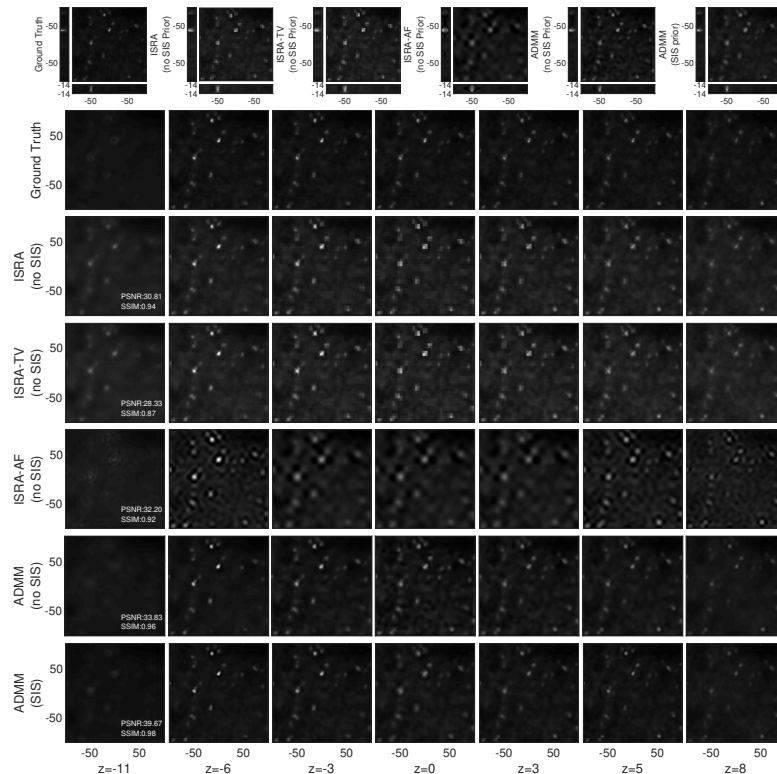


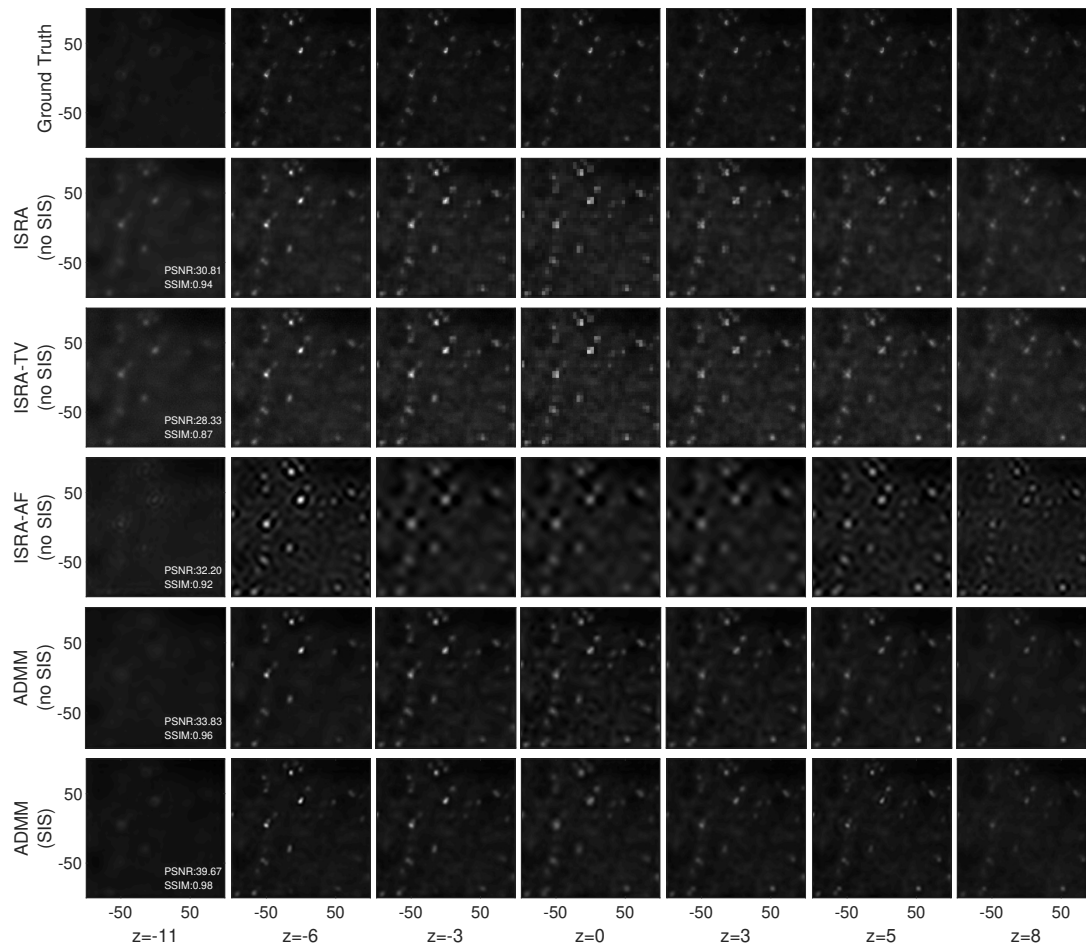
Volume Reconstruction from LF Data

- Further improvements are possible by adding further priors:

$$\begin{aligned} \min_{\mathbf{f}} \quad & \|\mathbf{H}_\delta \mathbf{S}_\varphi \mathbf{A}_\varphi \mathbf{f} - \mathbf{g}\|_2^2 + \|\mathbf{D}_x^n \mathbf{f}\|_1 + \|\mathbf{D}_y^n \mathbf{f}\|_1 + \|\mathbf{D}_z^n \mathbf{f}\|_1 \\ \text{s.t.} \quad & \mathbf{f} \geq \mathbf{0}, \end{aligned}$$

- Optimization solved using ADMM

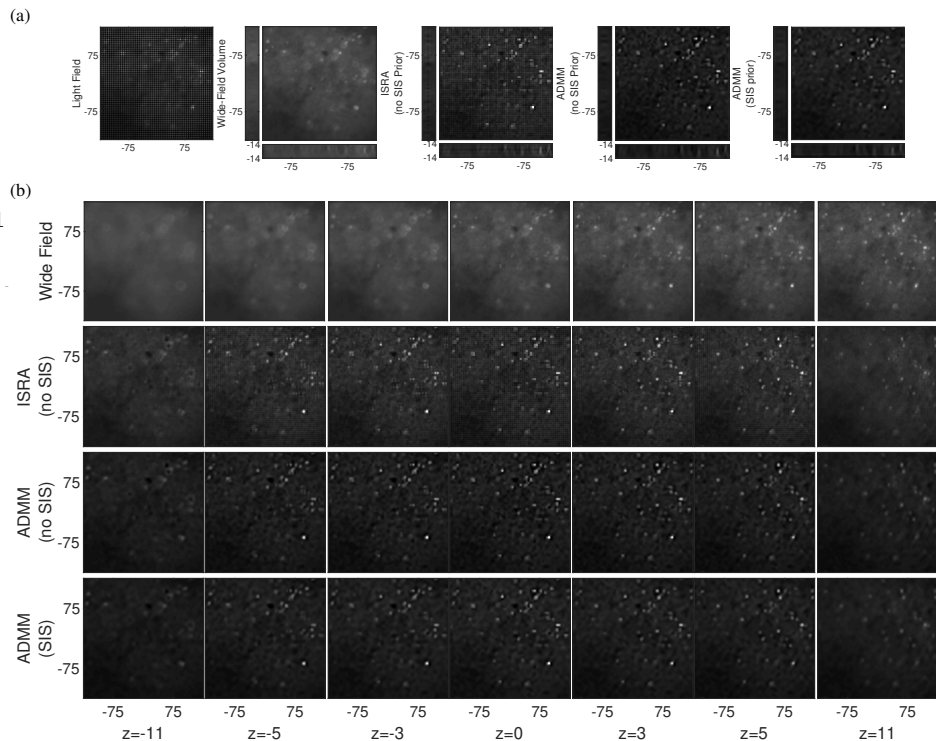


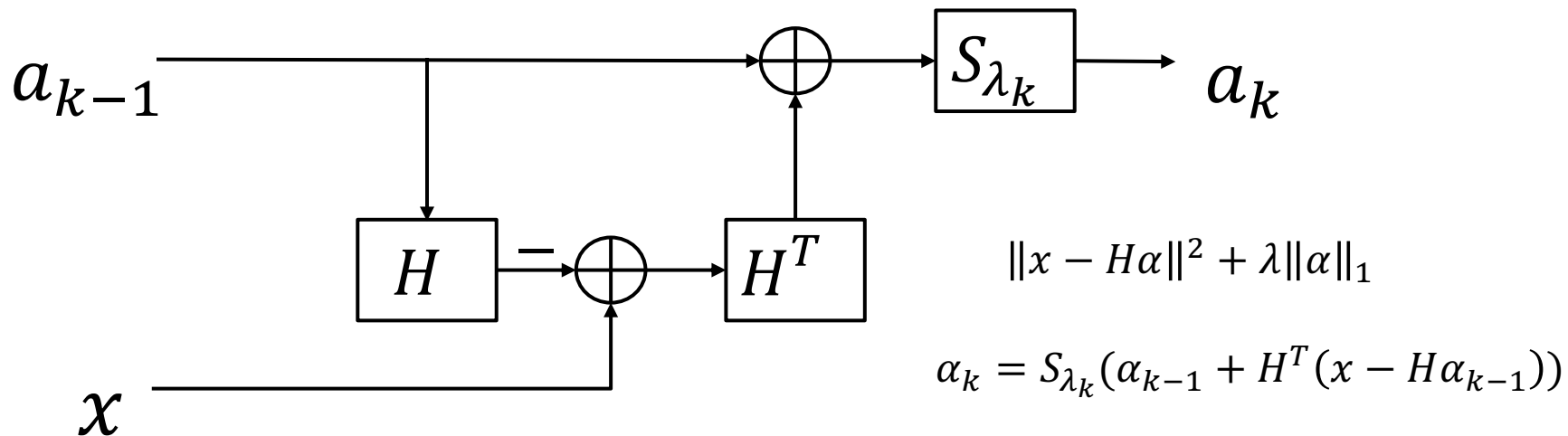


- Further improvements are possible by adding further priors:

$$\begin{aligned} \min_{\mathbf{f}} \quad & \| \mathbf{H}_\delta \mathbf{S}_\varphi \mathbf{A}_\varphi \mathbf{f} - \mathbf{g} \|_2^2 + \| \mathbf{D}_x^n \mathbf{f} \|_1 + \| \mathbf{D}_y^n \mathbf{f} \|_1 + \| \mathbf{D}_z^n \mathbf{f} \|_1 \\ \text{s.t.} \quad & \mathbf{f} \geq \mathbf{0}, \end{aligned}$$

- Optimization solved using ADMM



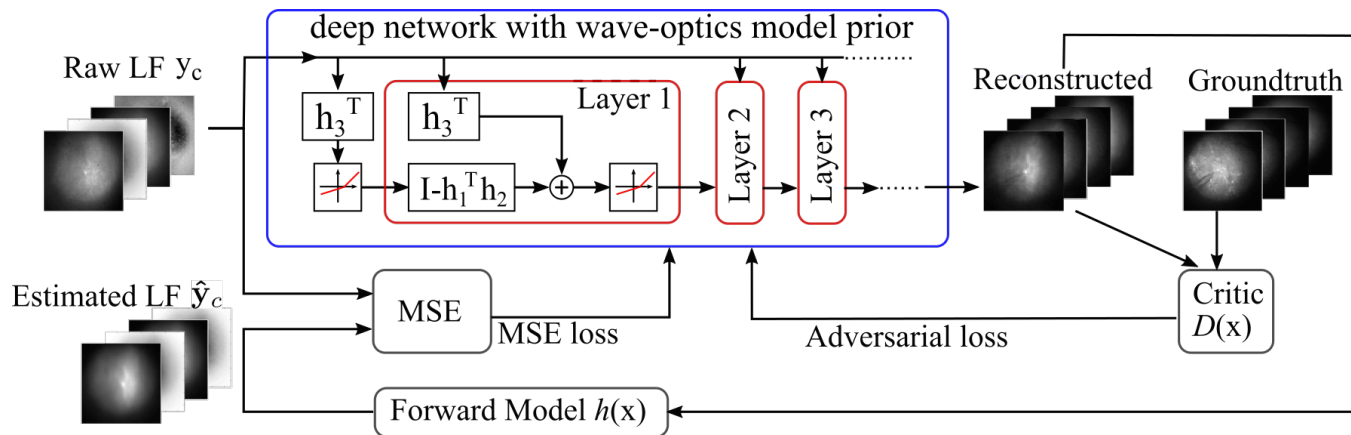


Inspired by LISTA¹, we “unfold” this iteration to obtain a deep network

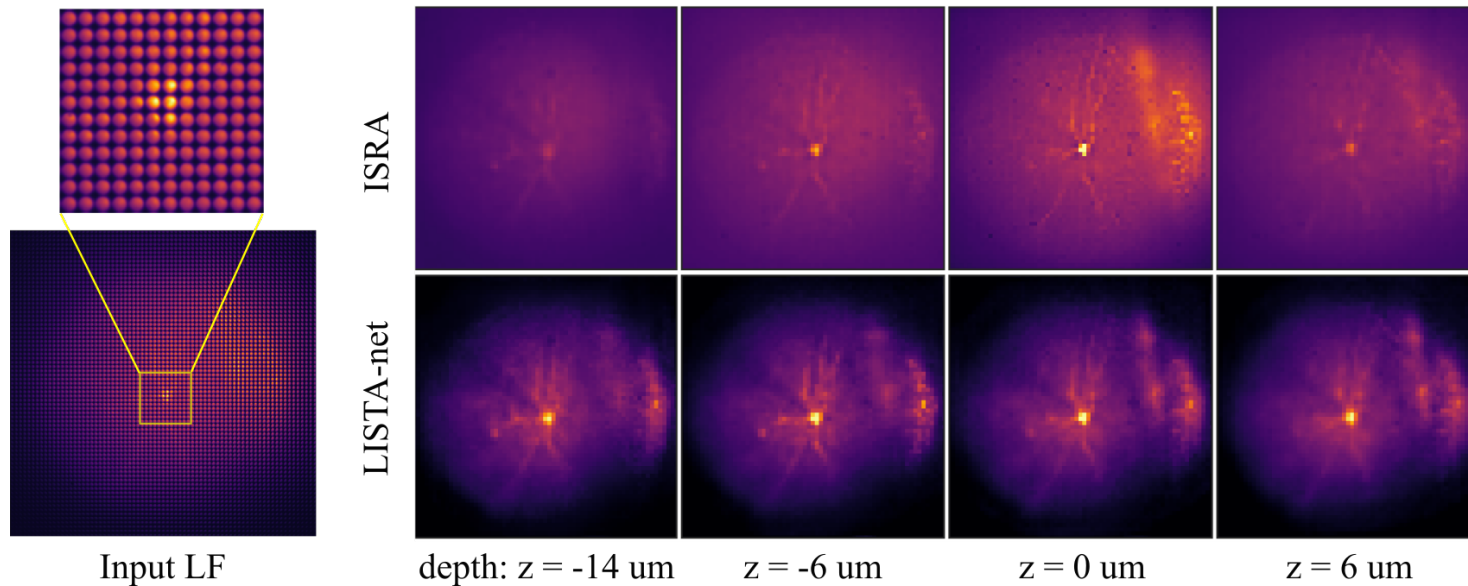
¹Gregor Karol and LeCunYann, “Learning fast approximations of sparse coding”, Proceedings of the 27th International Conference on International Conference on Machine Learning, 2010

On-going: Learning-based Reconstruction

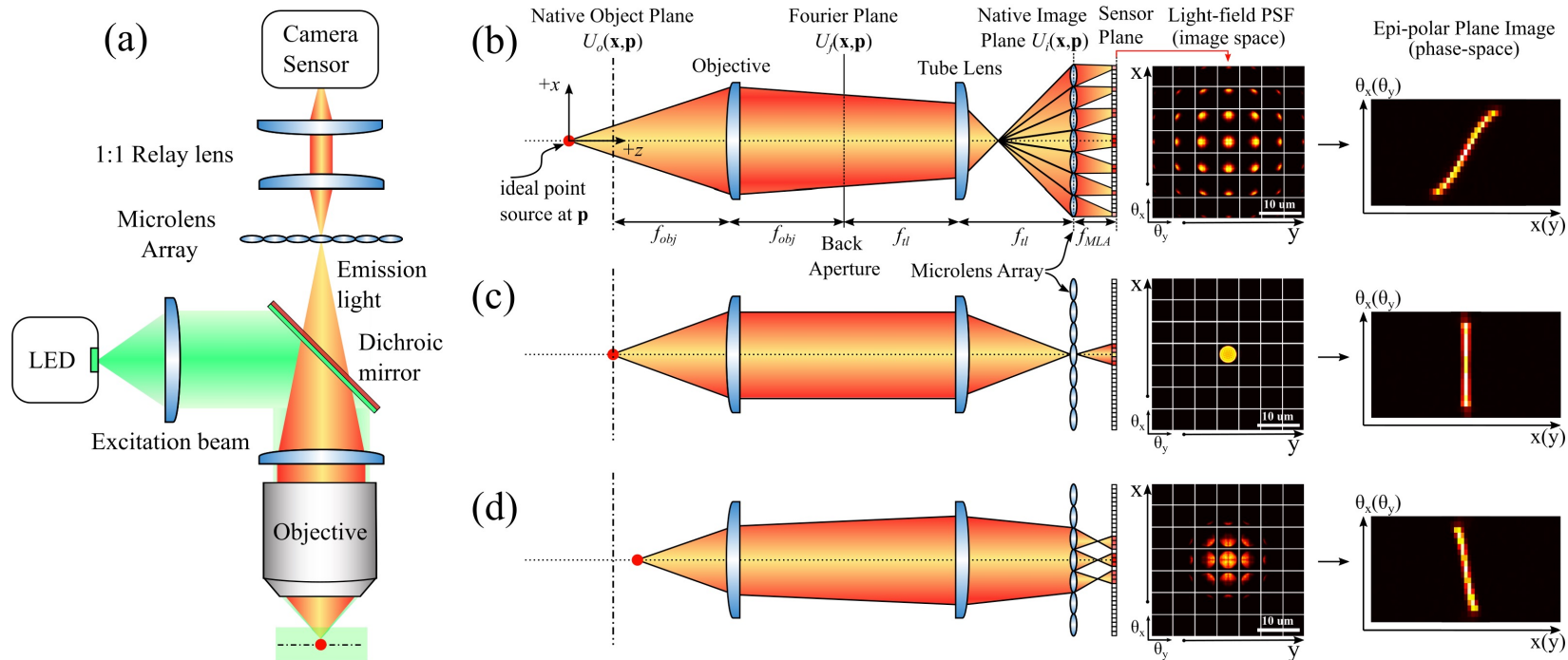
- Combines the light-field wave-optics model with Learned Iterative Shrinkage-Thresholding Algorithm (LISTA)
- Un-paired data calls for adversarial network



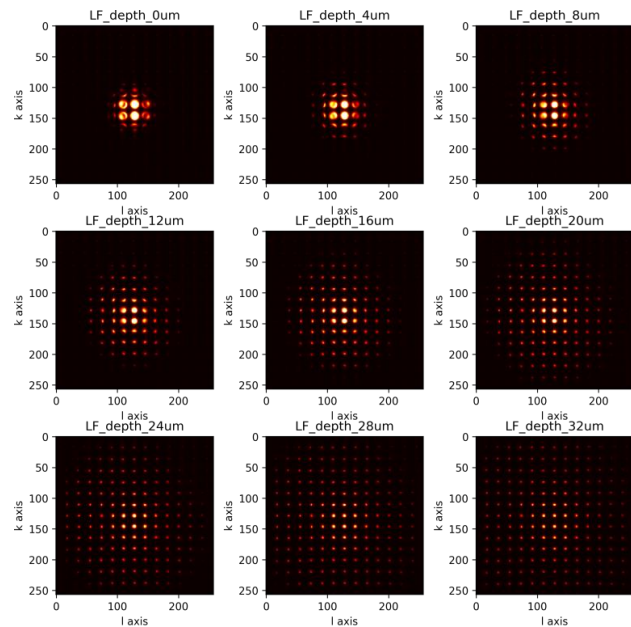
Learning-based Reconstruction- Results



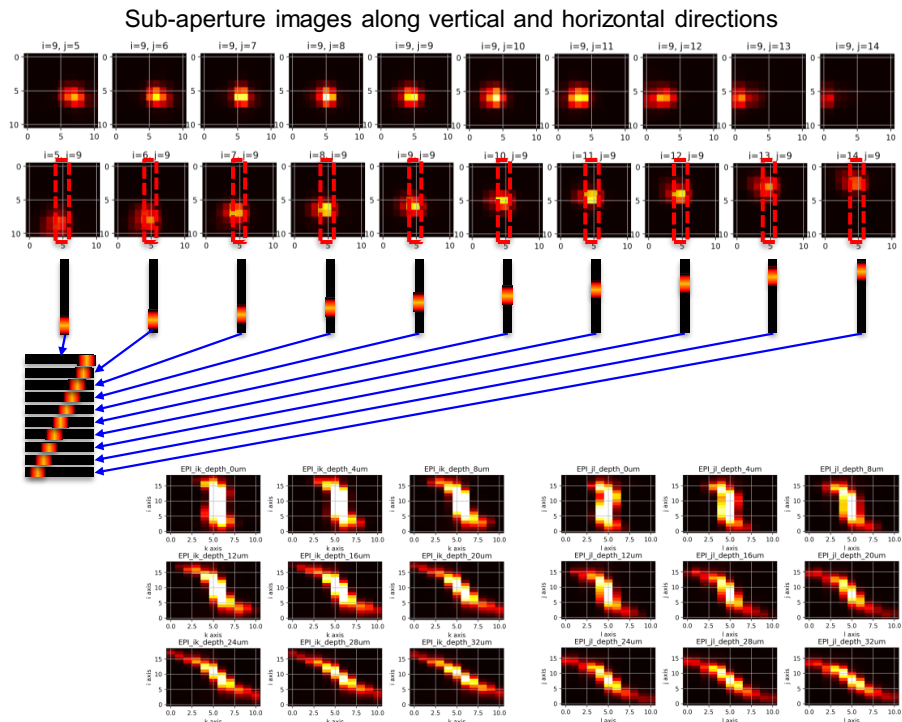
Localization of Neurons using LFM



Real Lightfield Images and EPIs

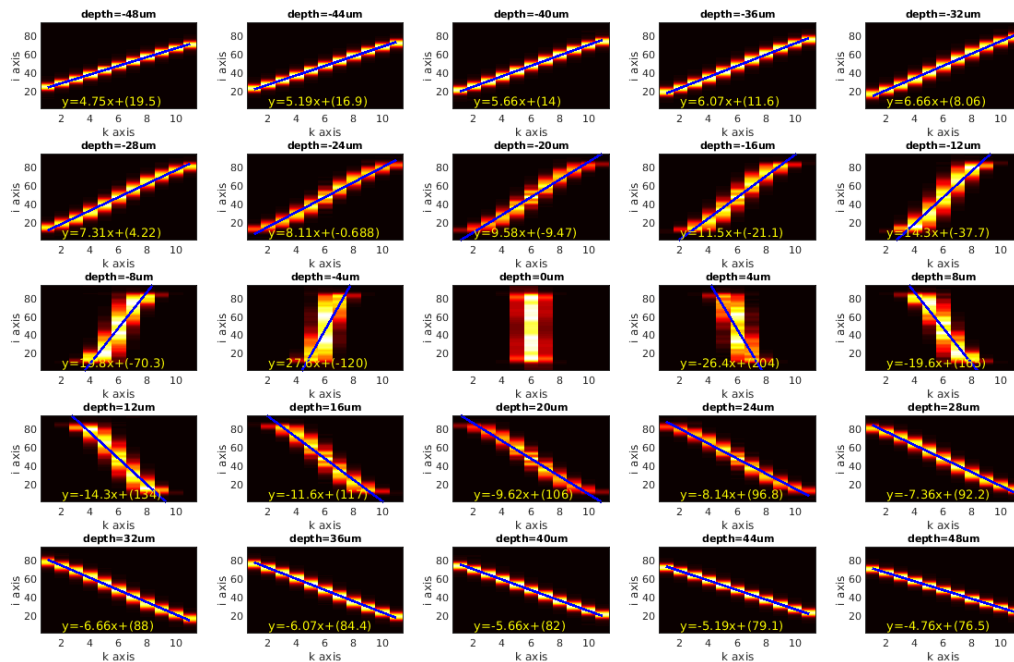


Real LFM for a bead in different depths ranging from 0 to 32 μm



EPIs from real LFM data. i - k direction (left) and j - l direction (right)

Dictionary of EPI from Simulated Lightfield Microscope



Simulated EPI dictionary. Each atom corresponds to a specific depth

We develop a convolutional sparse coding algorithm to decompose the input EPI into latent factors to estimate depth and spatial locations.

Objective in image domain:

$$\min_{\mathbf{z}} \frac{1}{2} \|\mathbf{Y} - \sum_{m=1}^M \mathbf{d}_m * \mathbf{z}_m\|_2^2 + \beta \sum_{m=1}^M \|\mathbf{z}_m\|_1$$

Objective in Fourier domain:

$$\min_{\mathbf{z}_m} \frac{1}{2} \|\hat{\mathbf{Y}} - \sum_{m=1}^M \hat{\mathbf{d}}_m \odot \hat{\mathbf{z}}_m\|_2^2 + \beta \sum_{m=1}^M \|\mathbf{z}_m\|_1$$

Objective in matrix format:

$$\min_{\mathbf{Z}} \frac{1}{2} \|\hat{\mathbf{Y}} - \hat{\mathbf{D}}\hat{\mathbf{Z}}\|_2^2 + \beta \|\mathbf{Z}\|_1$$

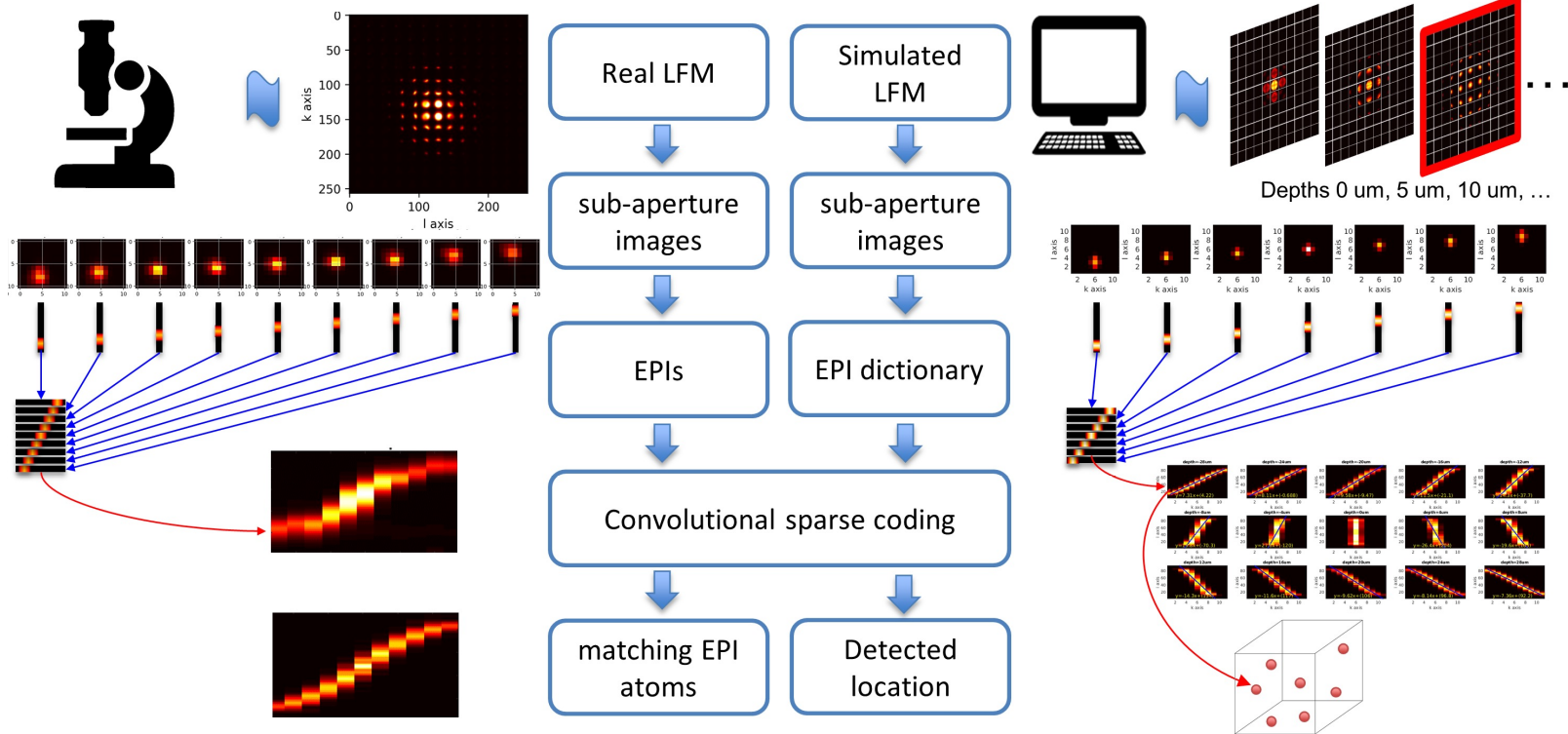
Lagrangian

$$\mathcal{L}(\mathbf{Z}, \mathbf{T}, \gamma) = \frac{1}{2} \|\mathbf{Y} - \mathbf{D}\mathbf{Z}\|_2^2 + \beta \|\mathbf{T}\|_1 + \gamma^\top (\mathbf{Z} - \mathbf{T}) + \frac{\mu}{2} \|\mathbf{Z} - \mathbf{T}\|_2^2$$

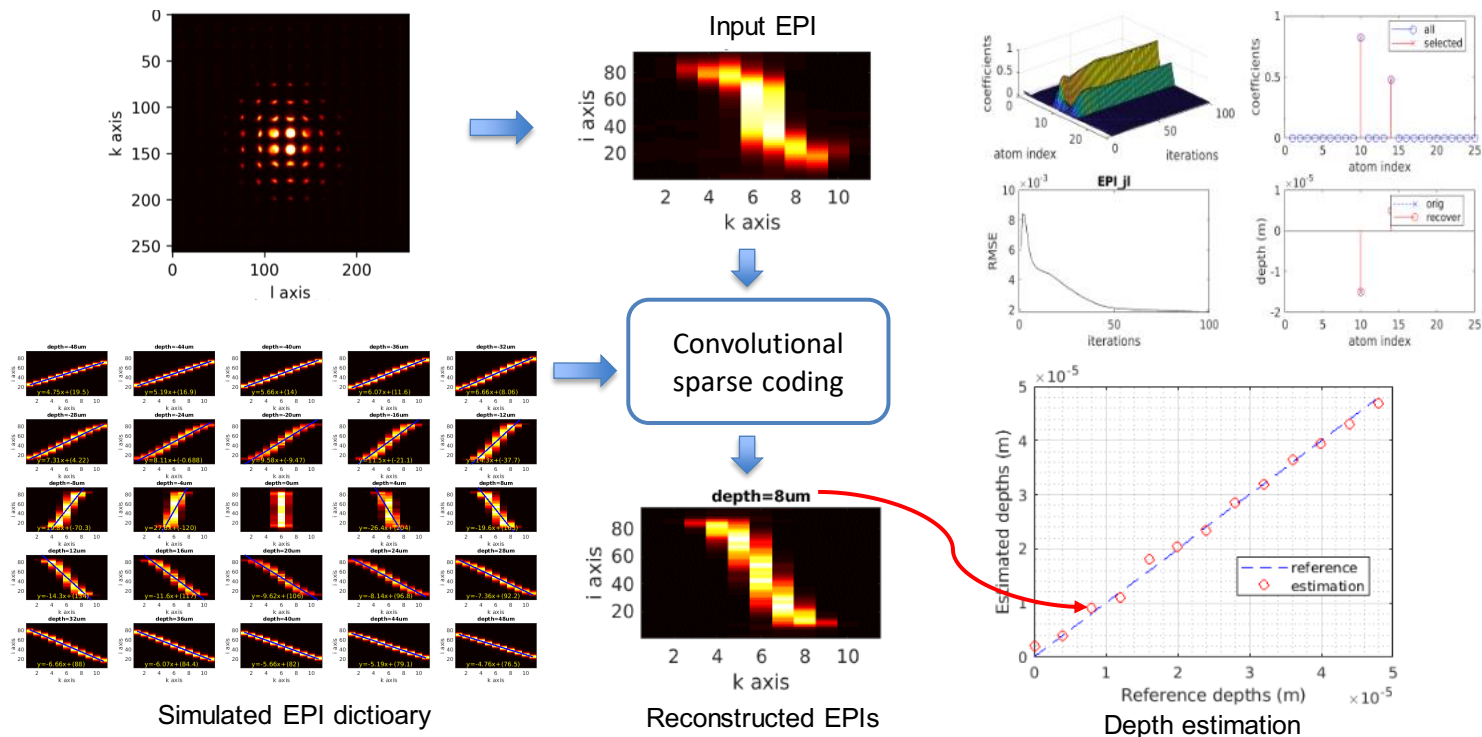
ADMM algorithm for solving CSC

$$\begin{aligned} \mathbf{Z}^{(i+1)} &= \arg \min_{\mathbf{Z}} \mathcal{L}(\mathbf{Z}, \mathbf{T}^{(i)}, \gamma^{(i)}) \\ &= \mathcal{F}^{-1} \{ (\hat{\mathbf{D}}^\top \hat{\mathbf{D}} + \mu \mathbf{I})^{-1} (\hat{\mathbf{D}}^\top \hat{\mathbf{Y}} - \hat{\gamma} + \mu \hat{\mathbf{T}}^{(i)}) \} \\ \mathbf{T}^{(i+1)} &= \arg \min_{\mathbf{T}} \mathcal{L}(\mathbf{Z}^{(i+1)}, \mathbf{T}, \gamma^{(i)}) \\ &= \mathbf{S}_{\beta/\mu}(\mathbf{Z}^{(i+1)}) + \gamma^{(i)}/\mu \\ \gamma^{(i+1)} &= \arg \min_{\gamma} \mathcal{L}(\mathbf{Z}^{(i+1)}, \mathbf{T}^{(i+1)}, \gamma) \\ &= \gamma^{(i)} + \mu(\mathbf{Z}^{(i+1)} - \mathbf{T}^{(i+1)}) \end{aligned}$$

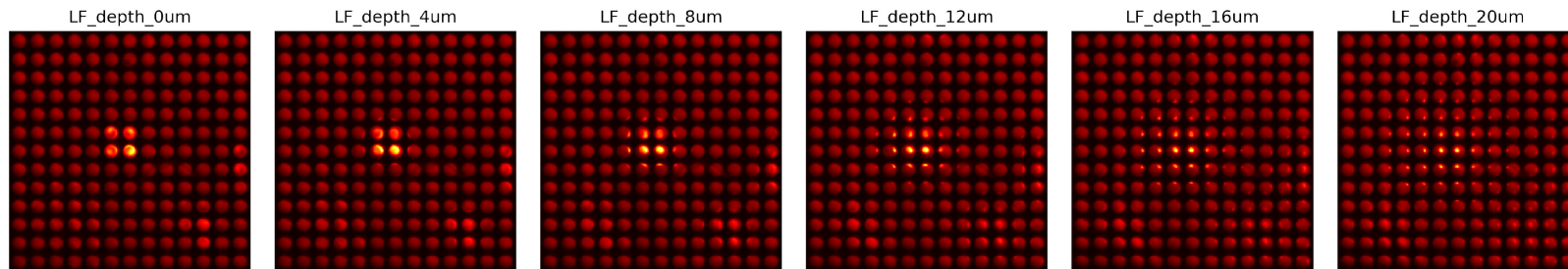
Neuron Localization Approach



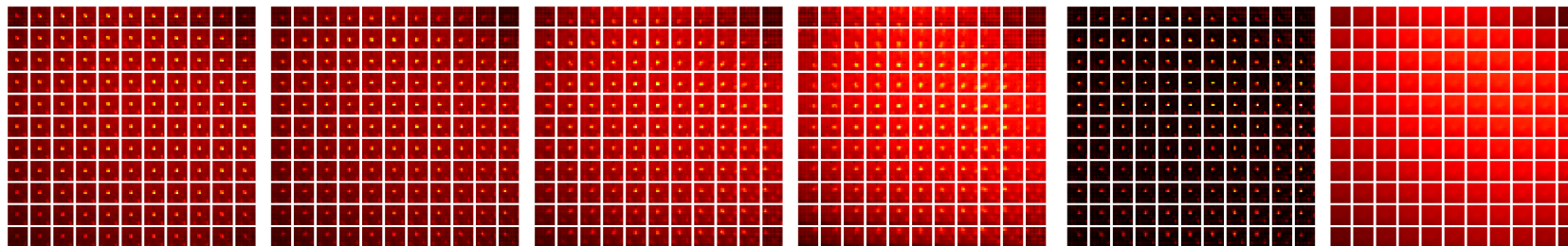
Location Estimation Algorithm



Numerical Results



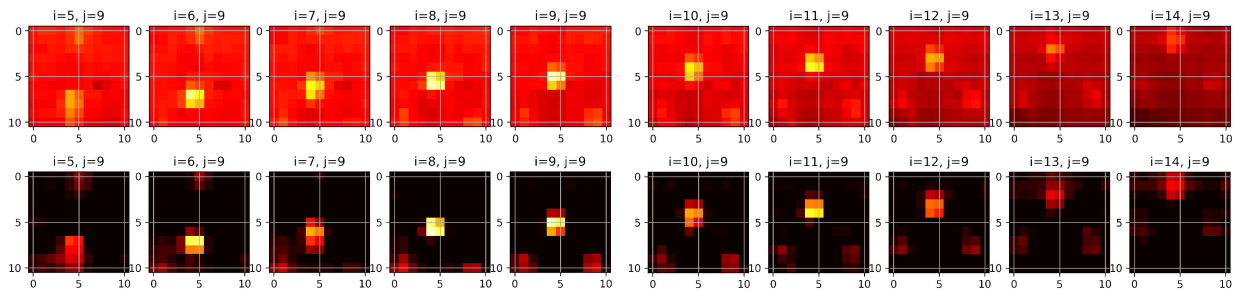
(a) Raw LFM data for a neuronal cell at different depths away from the focal plane.



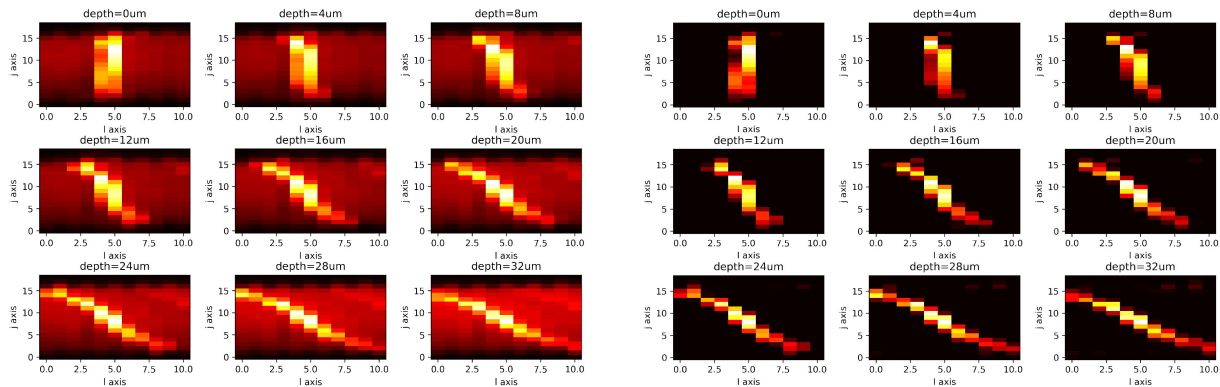
(b) Sub-aperture image arrays for depth 0, 12, 24 and 36 μm, respectively.

(c) Foreground and Background at depth 12 μm

Numerical Results



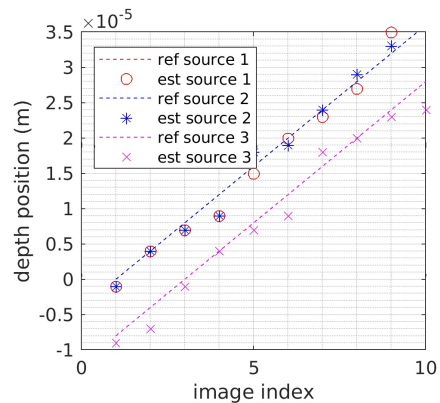
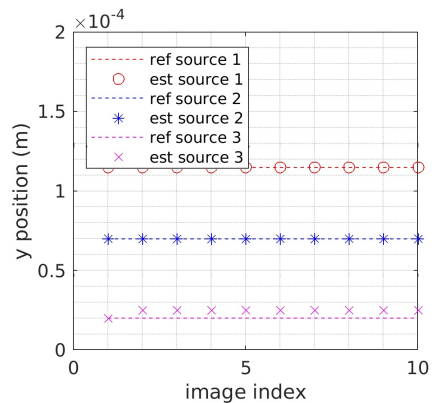
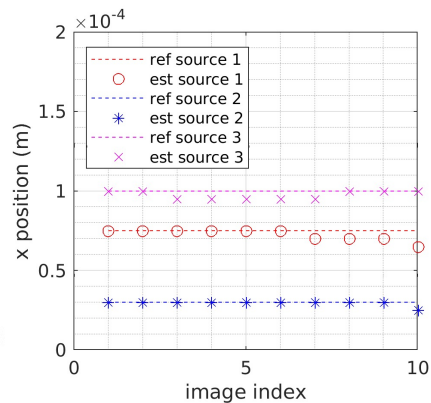
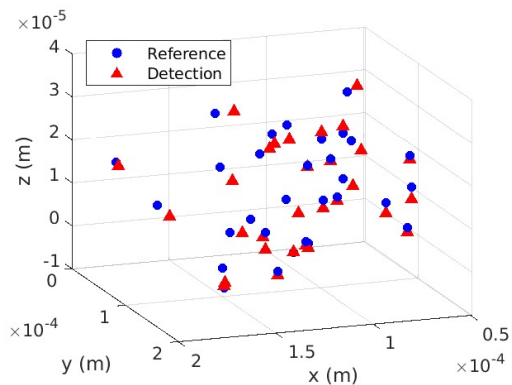
(d) The central column of the sub-aperture image array at depth $36 \mu\text{m}$. View changes from down to up. Above: with background. Below: background is removed.



(e) Constructed EPIs in the $j-l$ space.

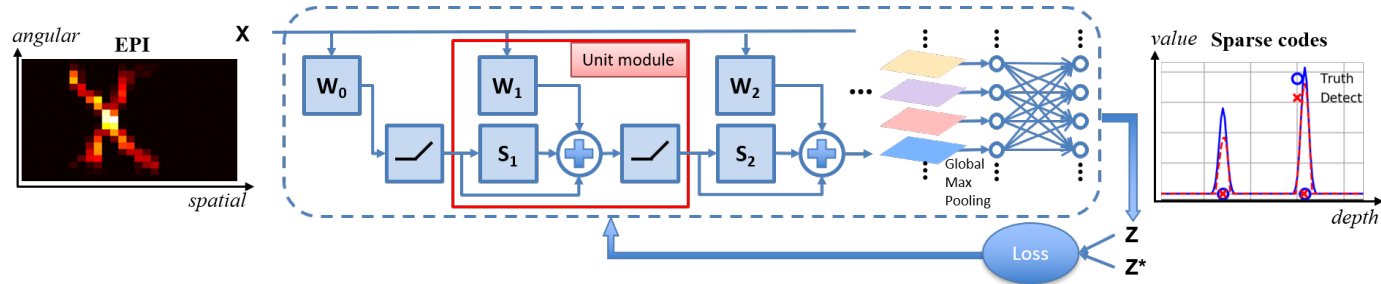
Purified EPIs in the $j-l$ space without background.

Numerical Results

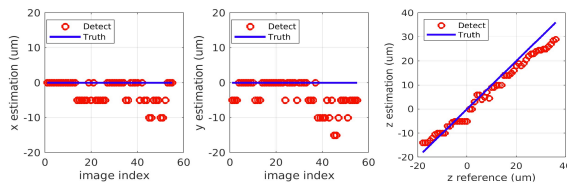


On-going work – CISTA for localization

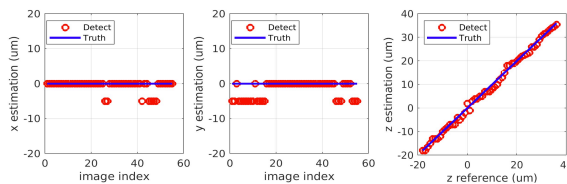
- The convolutional sparse model leads naturally to an iterative optimization strategy (ISTA) that can be unfolded
- Training based on synthetic data obtained using the Broxton forward model



On-going work – CISTA for localization



(a) Localization performance of phase-space method [6, 8]. RMSE for x, y, z position detection is 4.05, 5.48, 3.41 μm , respectively.



(b) Localization performance of CSC approach [9]. RMSE for x, y, z position detection is 1.78, 2.94, 1.14 μm , respectively.



(c) Localization performance of the proposed CISTA-net. RMSE for x, y, z position detection is 1.60, 1.98, 0.82 μm , respectively.

Conclusions

- Light field systems can have an impact in neuroscience because of the crucial trade-off between resolution in time and space
 - Light field microscopy brings unique challenges e.g., wave optics
 - In neuroscience applications, data is sparse and occlusion is negligible
 - Understanding the physics of the problem is crucial
 - Learning with labelled data is challenging
-

Thank you!

On Light-Field Microscopy and Neuroscience

- P. Song, H. Verinaz Jadan, C. Howe, P. Quicke, A. Foust and P.L. Dragotti, “3D localization for light-field microscopy via convolutional sparse coding on epipolar images”, IEEE Transactions on Computational Imaging, Vol:6, pages:1017-1032, 2020.
- H. Verinaz Jadan, P. Song, C. Howe, A. Foust and P.L. Dragotti, “Artifact-free 3D Reconstruction for Light Field Microscopy”, IEEE Transactions on Computational Imaging, submitted 2021.
- P. Song, H. Verinaz Jadan, C. Howe, P. Quicke, A. Foust and P.L. Dragotti, Light-field microscopy for optical imaging of neuronal activity, IEEE Signal Processing Magazine, submitted 2021.